IEEE Robotics and Automation Letters (RA-L) paper, presented at ICRA 2026, Vienna, Austria. Cite as RA-L paper.

Nullspace Adaptive Velocity Controller for Ground Vehicles: Theory and Experimental Evaluation

Allan H. Elsberry[1,2], Jeremy J. Dawkins[2], and Louis L. Whitcomb[1]

***Abstract*—We report a novel stable Model-Based Adaptive Velocity Tracking Controller (AVTC) for ground vehicles capable of asymptotically exactly tracking longitudinal and yaw reference velocities and simultaneously adaptively identifying unknown plant parameters and actuator parameters. The reported AVTC is developed for velocity control of the commonly accepted three degree-of-freedom second-order dynamic "bicycle" model for ground vehicles.**

A Lyapunov analysis shows asymptotic stability of the velocity tracking error in longitudinal and yaw velocities, boundedness of all signals, and convergence of the adaptive parameter estimates. A performance evaluation of the proposed AVTC is reported including numerical simulation evaluation and experimental evaluation that corroborates the analytical predictions of stability and tracking, and compares its performance to its non-adaptive counterpart and two alternative controllers.

AVTC only requires body-frame velocities and control input signals, and robustly detects, quantitatively identifies, and compensates dynamically in real-time for faults arising from changes to plant, actuator, and environmental parameters during operations.

***Index Terms*—Robust/adaptive control, underactuated robots, model parameter identification, model-based control**

I. Introduction

THIS letter addresses the problem of stable trajectory-tracking velocity control for ground vehicles for which plant parameters (such as mass, moment-of-inertia, payload, rolling resistance) and actuator parameters (such as motor torque constants and tire cornering stiffness values) are *a priori* unknown. Fixed model-based control approaches to this problem require previous identification of the ground vehicle plant and model parameter values, and their stability and performance may degrade if model parameters are not known exactly, or change during ground vehicle operation.

This letter reports a novel stable model-based Adaptive Velocity Tracking Controller (AVTC) for underactuated ground vehicles capable of asymptotically exactly tracking time-varying reference longitudinal and yaw velocities and simultaneously adaptively identifying unknown plant parameters and actuator parameters. The reported AVTC is developed for velocity control of the commonly accepted Three Degree of Freedom (3-DOF) second-order dynamic "bicycle" model for ground vehicles.

We report a mathematical stability analysis showing asymptotic stability of the velocity tracking error in longitudinal and yaw velocities, boundedness of all signals, and convergence of the adaptive parameter estimates.

We report the first performance evaluation of the proposed AVTC including numerical simulation evaluation and experimental evaluation, which corroborate the analytical predictions of stability and performance, and compares its performance to its non-adaptive counterpart and two alternative controllers.

AVTC provides the following advantages:

1. Stable Tracking Control in Presence of Unknown, Changing, and Faulty Plant and Actuator Parameters: Adaptive model-based control algorithms can provide fault-tolerant control that adapts to changes and faults in vehicle parameters (e.g.: changes in mass or inertia due to mission payload, or changes in tire cornering stiffness due to tire wear) and environment interaction (e.g rolling resistance and cornering stiffness) to provide more accurate and robust control in comparison to non-adaptive control [13].

2. Mathematical Stability and Performance Guarantees: The proposed model-based AVTC guarantees real-time online stability and convergence of tracking error and parameter estimates, in contrast to the three other controllers evaluated herein which do not estimate plant or actuator parameters online, and two of which do not have stability proofs. It is also in contrast to general Machine Learning/Artificial Intelligence (ML/AI) approaches, which may not mathematically guarantee stability, require large training data sets, and do not provide short-term real-time online learning.

3. Safety: Adaptive control approaches can provide more stable control that adjusts to changing vehicle and environmental parameters when operating on slippery road surfaces [1] or performing collision avoidance maneuvers [2].

4. Fault Detection, Isolation, and Compensation: Online quantitative identification of changes in vehicle plant, actuator, and environment parameters enables real-time fault detection, fault-isolation, and fault-tolerant control [16].

5. Minimal Instrumentation Requirements: The proposed AVTC requires the signals of vehicle body-frame velocities and control input signals only, in contrast to model identification techniques such as least-squares that additionally require the signal of vehicle body-frame accelerations.

The remainder of this letter is organized as follows: Section II reviews relevant previous literature. Section III introduces

Manuscript received: January, 6, 2025; Revised March, 24, 2025; Accepted April, 29, 2025.

This paper was recommended for publication by IEEE Robotics and Automation Letters Editor Cosimo Della Santina upon evaluation of the Associate Editor and Reviewers' comments. This work was supported by the U.S. Navy (Elsberry, Dawkins), the JHU William F. Ward, Jr. Fellowship (Elsberry), and the National Science Foundation under Award 1909182 (Whitcomb).

[1]Department of Mechanical Engineering Johns Hopkins University Baltimore, MD 21218, USA. llw@jhu.edu

[2]Department of Weapons, Robotics, and Control Engineering United States Naval Academy, Annapolis, MD 21401, USA. elsberry@usna.edu, dawkins@usna.edu. The views expressed in this document are those of the authors and do not reflect the official policy or position of the U.S. Naval Academy, Dept. of the Navy, Dept. of War, or the U.S. Government.

the dynamical vehicle plant and actuator model, and the AVTC controller. Section IV reports numerical simulation results, tracking performance, and convergence of the AVTC estimated parameter values to the true parameter values. Section V reports a comparative experimental evaluation of AVTC and three other controllers with a $1/10^{th}$ scale ground vehicle. Section VI summarizes and concludes.

II. Literature Review

The most common reported approaches to estimate ground vehicle model parameters from experimental data are through Least Squares (LS) regression, the extended Kalman filter (EKF), or the Unscented Kalman filter (UKF).

In [22] the authors use LS to estimate the yaw moment of inertia. In [10] the authors use Recursive Least Squares (RLS) to estimate the vehicle mass and yaw moment of inertia. Both approaches require measurements of lateral acceleration and yaw angular acceleration. While their studies did not include experimental validation, they demonstrated the feasibility of estimating geometric parameters using these methods. For many vehicle control applications, estimates of the tire forces are required to optimize performance. In [3] the authors report a linearized RLS algorithm for online estimation of tire-road friction coefficients, utilizing an EKF with the vehicle model to estimate the tire forces and feed those estimates to the RLS algorithm. In [4] a LS approach is reported for estimating tire cornering stiffness during operation with batch processing.

In [20] the authors report an EKF algorithm to act as an observer for vehicle states and to estimate the mass parameter of a passenger vehicle. This approach is shown to be effective in estimating the mass parameter of the vehicle and as the mass parameter improves, the state estimation observer also improves. In [8] the authors utilized two coupled UKFs to estimate the sprung mass and the moments of inertia of the roll and yaw of the vehicle; experimental data from a passenger car was used to validate this approach.

In most previous studies, parameter estimation is decoupled from the controller. However, the authors of [12] show in a simulation study that using RLS, the estimates of yaw moment of inertia and cornering stiffness can be used with an H_∞ controller to improve the robustness of yaw rate tracking performance. In [13] the authors also report the performance of a RLS algorithm to estimate the tire cornering stiffness coefficients and to estimate the parameters of a dynamics model used for Model Predictive Control (MPC).

LS parameter estimation from experimental data of second-order mechanical systems such as ground vehicles requires three sets of instrumented signals: linear and angular body-frame velocity, linear and angular body-frame acceleration, and control inputs such as motor commands and steering commands. Measurement of body-frame linear acceleration is complicated by the large 1 g gravity signal.

More recently, ML/AI approaches have been studied for learning the vehicle dynamics models and control policies from experimental data. In [18] the authors report and compare several deep reinforcement learning methods to control autonomous vehicles to include Q learning and Deep Deterministic Policy Gradient (DDPG) methods. While these approaches can be effective, [11], these methods require significant data collection and computational resources, which may not be available for online updates. Most ML/AI approaches do not mathematically guarantee stability, require large training data sets that ideally cover the entire operating range of the vehicle [14], and do not provide short-term real-time online learning.

In [9] the authors acknowledge the limitations of online ML/AI and report a vehicle controller that combines a simplified bicycle dynamics model for a path-following MPC. The simplified model allows for MPC with limited computational resources, and uses a Gaussian process regression to learn model error in different operating envelopes.

In [15] a nullspace adaptive trajectory tracking controller for fully-actuated 6-DOF underwater vehicles is reported. This study reports a mathematical stability proof and numerical simulations showing asymptotically stable convergence of position and velocity trajectory tracking error. Full 6-DOF trajectory tracking is generally not possible for underactuated vehicles. As examined in [21], control of underactuated systems often requires a different problem formulation and control approach than for fully-actuated systems.

In [5] a Nullspace Adaptive Identification (NS-AID) algorithm is reported that estimates plant and actuator parameters including mass and tire cornering stiffness coefficients for an underactuated ground vehicle that requires only vehicle body-velocity signals and control input signals.

The AVTC reported herein builds on the NS-AID algorithm reported in [5]. This AVTC controller is capable of estimating plant and actuator parameters online in real-time and also provides asymptotically stable longitudinal velocity and yaw rate tracking control. Unlike LS parameter estimation methods, the AVTC algorithm does not require acceleration signals. Unlike ML/AI approaches AVTC does not require large training data sets, can provide real-time online model parameter identification with minimal computational resources, and AVTC is proven mathematically to provide stable online parameter estimation and asymptotically stable velocity tracking.

III. Ground Vehicle Model and Adaptive Velocity Tracking Controller

Section III-A presents a 3-DOF ground vehicle dynamical model, Section III-B reports a non-adaptive model-based controller for known plant and actuator parameter values, Section III-C reports the AVTC controller, and Section III-E reports an AVTC stability analysis.

A. Dynamic Ground Vehicle "Bicycle" Model

A 3-DOF ground vehicle dynamical model in which the lateral and yaw dynamics are based on the widely accepted "bicycle model" [19] takes the form

$$\ddot{x} = K_t \frac{I_m}{m} - \frac{C_{rr}\dot{x}}{m} + \dot{y}\dot{\psi} \tag{1}$$

$$\ddot{\psi} = -\frac{C_{\alpha f} l_f - C_{\alpha r} l_r}{J_z \dot{x}} \dot{y} - \frac{C_{\alpha f} l_f^2 + C_{\alpha r} l_r^2}{J_z \dot{x}} \dot{\psi} + \frac{C_{\alpha f} l_f}{J_z} \delta \tag{2}$$

$$\ddot{y} = -\frac{C_{\alpha f} + C_{\alpha r}}{m \dot{x}} \dot{y} - \frac{C_{\alpha f} l_f - C_{\alpha r} l_r}{m \dot{x}} \dot{\psi} + \frac{C_{\alpha f}}{m} \delta - \dot{x}\dot{\psi} \tag{3}$$

where the longitudinal dynamics (1) has the control input of motor current, I_m [A] , and the lateral dynamics (3) and yaw dynamics (2) have the control input of front wheel steering angle, δ [rad]. Eq. (2) and (3) represent the bicycle dynamics

TABLE I: State Variables and Control Inputs

$\dot{x}$	Longitudinal velocity	m/s
$\dot{y}$	Lateral velocity	m/s
$\dot{\psi}$	Yaw rate	rad/s
I_m	Motor Current	A
δ	Front tire steering angle	rad

TABLE II: Plant (P) and Actuator (A) Model Parameters

l_f	Distance, center of mass to front wheel	m	P
l_r	Distance, center of mass to rear wheel	m	P
m	Vehicle mass	kg	P
J_z	z-axis moment of inertia	$kg \cdot m^2$	P
K_t	Motor drive-train torque constant	N/A	A
C_{rr}	Rolling resistance coefficient	$N \cdot s/m$	P
$C_{\alpha f}$	Front tire cornering stiffness	N/rad	A
$C_{\alpha r}$	Rear tire cornering stiffness	N/rad	P
C_Δ	$C_{\alpha f} - C_{\alpha r}$	N/rad	P
C_Σ	$C_{\alpha f} + C_{\alpha r}$	N/rad	P

model as reported in [19]. Tables I and II define system variables and plant and actuator model parameters. The model parameters, C_Σ and C_Δ, can be defined as

$$C_\Sigma = C_{\alpha f} + C_{\alpha r} \qquad C_\Delta = C_{\alpha f} - C_{\alpha r}, \tag{4}$$

and substituted into (2) and (3) for simplification. Additionally, the center of mass for our vehicle is located at the center of the longitudinal axis such that $l_f = l_r = l$, thus

$$\ddot{x} = K_t \frac{I_m}{m} - \frac{C_{rr}\dot{x}}{m} + \dot{y}\dot{\psi} \tag{5}$$

$$\ddot{\psi} = -\frac{C_\Delta l}{J_z \dot{x}}\dot{y} - \frac{C_\Sigma l^2}{J_z \dot{x}}\dot{\psi} + \frac{C_{\alpha f} l}{J_z}\delta \tag{6}$$

$$\ddot{y} = -\frac{C_\Sigma}{m\dot{x}}\dot{y} - \frac{C_\Delta l}{m\dot{x}}\dot{\psi} + \frac{C_{\alpha f}}{m}\delta - \dot{x}\dot{\psi}. \tag{7}$$

We note that $C_{\alpha f}$ is still present in the simplified equations as an actuator model parameter for a linear mapping between the steering control input signal and the actual steering angle.

Defining the velocity state vector as

$$\dot{z} \triangleq [\ \dot{x} \quad \dot{\psi} \quad \dot{y}\ ]^T \in \mathbb{R}^3 \tag{8}$$

results in the final body-frame velocity dynamics of

$$\ddot{z} = \begin{bmatrix} \ddot{x} \\ \ddot{\psi} \\ \ddot{y} \end{bmatrix} = \begin{bmatrix} K_t \frac{I_m}{m} - \frac{C_{rr}\dot{x}}{m} + \dot{y}\dot{\psi} \\ -\frac{C_\Delta l}{J_z \dot{x}}\dot{y} - \frac{C_\Sigma l^2}{J_z \dot{x}}\dot{\psi} + \frac{C_{\alpha f} l}{J_z}\delta \\ -\frac{C_\Sigma}{m\dot{x}}\dot{y} - \frac{C_\Delta l}{m\dot{x}}\dot{\psi} + \frac{C_{\alpha f}}{m}\delta - \dot{x}\dot{\psi} \end{bmatrix}. \tag{9}$$

B. Non-Adaptive Velocity Tracking Controller (VTC)

This Section reports the design of a non-adaptive model-based controller capable of tracking longitudinal and yaw velocity reference signals with known vehicle plant and actuator parameters. Defining the parameter vector, $\theta \in \mathbb{R}^{7\times 1}$, as

$$\theta \triangleq \begin{bmatrix} m, & J_z, & K_t, & C_{rr}, & C_{\alpha f}, & C_\Sigma, & C_\Delta \end{bmatrix}^T \tag{10}$$

where all elements are real, and all elements except C_Δ are positive, and defining the Positive Definite Diagonal (PDD) mass matrix, $M(\theta) \in \mathbb{R}^{3\times 3}$, as

$$M(\theta) \triangleq \begin{bmatrix} m & 0 & 0 \\ 0 & J_z & 0 \\ 0 & 0 & m \end{bmatrix} \tag{11}$$

and the control input vector, $u = [I_m \quad \delta]^T \in \mathbb{R}^{2\times 1}$, the system dynamics from (9) can be written in the form

$$\ddot{z} = M(\theta)^{-1}[f(\dot{z}, \theta) + BA(\theta)u] \tag{12}$$

where

$$f(\dot{z}, \theta) = \begin{bmatrix} -C_{rr}\dot{x} + m\dot{y}\dot{\psi} \\ -\dot{x}^{-1}(C_\Delta \dot{y} l - C_\Sigma \dot{\psi} l^2) \\ -\dot{x}^{-1}(C_\Sigma \dot{y} - C_\Delta \dot{\psi} l) - m\dot{\psi}\dot{x} \end{bmatrix} \tag{13}$$

and

$$B = \begin{bmatrix} 1 & 0 \\ 0 & l \\ 0 & 1 \end{bmatrix} \quad A(\theta) = \begin{bmatrix} K_t & 0 \\ 0 & C_{\alpha f} \end{bmatrix}. \tag{14}$$

The VTC controller is designed to track smooth, bounded, time-varying reference velocities in $\dot{x}_d(t)$ and $\dot{\psi}_d(t)$, with $\dot{y}_d(t) = 0$, which in the sequel, for simplicity, we will omit the explicit dependence on t. The desired state vector is

$$\dot{z}_d \triangleq [\dot{x}_d \quad \dot{\psi}_d \quad \dot{y}_d]^T. \tag{15}$$

The controller's objective is to control $\dot{x}(t)$ and $\dot{\psi}(t)$ to track, respectively, $\dot{x}_d(t)$ and $\dot{\psi}_d(t)$, with bounded $\dot{y}(t)$, thus we define the reduced-dimension state vector and plant model as

$$\dot{\tilde{z}} \triangleq \begin{bmatrix} \dot{x} & \dot{\psi} \end{bmatrix}^T \quad \ddot{\tilde{z}} \triangleq \begin{bmatrix} \ddot{x} & \ddot{\psi} \end{bmatrix}^T \tag{16}$$

$$\dot{\tilde{z}}_d \triangleq \begin{bmatrix} \dot{x}_d & \dot{\psi}_d \end{bmatrix}^T \quad \ddot{\tilde{z}}_d \triangleq \begin{bmatrix} \ddot{x}_d & \ddot{\psi}_d \end{bmatrix}^T \tag{17}$$

$$\overline{M}(\theta) \triangleq \begin{bmatrix} m & 0 \\ 0 & J_z \end{bmatrix} \quad \overline{B} \triangleq \begin{bmatrix} 1 & 0 \\ 0 & l \end{bmatrix} \tag{18}$$

$$\overline{f}(\dot{z}, \theta) \triangleq \begin{bmatrix} -C_{rr}\dot{x} + m\dot{y}\dot{\psi} \\ -\frac{1}{\dot{x}}(C_\Delta \dot{y} l + C_\Sigma \dot{\psi} l^2) \end{bmatrix}. \tag{19}$$

The tracking error coordinates are

$$\Delta\dot{z} \triangleq \dot{z} - \dot{z}_d \quad \Delta\ddot{z} \triangleq \ddot{z} - \ddot{z}_d \tag{20}$$

$$\Delta\dot{\tilde{z}} \triangleq \dot{\tilde{z}} - \dot{\tilde{z}}_d \quad \Delta\ddot{\tilde{z}} \triangleq \ddot{\tilde{z}} - \ddot{\tilde{z}}_d. \tag{21}$$

The dynamics for the reduced-dimension state vector $\dot{\tilde{z}}$ can be written as

$$\ddot{\tilde{z}} = \overline{M}^{-1}(\theta)[\overline{f}(\dot{z}, \theta) + \overline{B}A(\theta)u]. \tag{22}$$

The VTC for $\Delta\dot{\tilde{z}}$ for the ground vehicle (12) utilizing known plant and actuator parameter values, θ, takes the form

$$u = A^{-1}(\theta)\overline{B}^{-1}[\overline{M}(\theta)\ddot{\tilde{z}}_d - \overline{f}(\dot{z}, \theta)] - K_c \Delta\dot{\tilde{z}} \tag{23}$$

where $K_c \triangleq \text{diag}([k_{\dot{x}},\ k_{\dot{\psi}}]) \in \mathbb{R}^{2\times 2}$ is a PDD feedback gain matrix.

The term $[\overline{M}(\theta)\ddot{\tilde{z}}_d - \overline{f}(\dot{z}, \theta)]$ in (23) is linear in the parameter vector θ (10) and can be written as the product of θ and the regressor matrices $W_M(\ddot{\tilde{z}}_d) \in \mathbb{R}^{2\times 7}$ and $W_{\bar{f}} \in \mathbb{R}^{2\times 7}$ defined as, respectively,

$$W_{\bar{M}}(\ddot{\tilde{z}}_d) = D_\theta[\overline{M}(\theta)\ddot{\tilde{z}}_d], \quad W_{\bar{f}}(\dot{z}) = D_\theta[\overline{f}(\dot{z}, \theta)], \tag{24}$$

such that

$$\overline{M}(\theta)\ddot{\tilde{z}}_d = W_{\bar{M}}(\ddot{\tilde{z}}_d)\theta, \quad \overline{f}(\dot{z}, \theta) = W_{\bar{f}}(\dot{z})\theta \tag{25}$$

where D_θ is the Jacobian operator of its argument with respect to θ. Substituting (24) into (23) results in the form

$$u = A^{-1}(\theta)\overline{B}^{-1}[W_{\bar{M}}(\ddot{\tilde{z}}_d) - W_{\bar{f}}(\dot{z})]\theta - K_c \Delta\dot{\tilde{z}}. \tag{26}$$

Defining the control regressor $W_c(\ddot{\tilde{z}}_d, \dot{z}) \in \mathbb{R}^{2\times 7}$ as

$$W_c(\ddot{\tilde{z}}_d, \dot{z}) \triangleq W_{\bar{M}}(\ddot{\tilde{z}}_d) - W_{\bar{f}}(\dot{z}), \tag{27}$$

the control law (26) can be written in regressor form as

$$u = A^{-1}(\theta)\overline{B}^{-1}W_c(\ddot{\tilde{z}}_d, \dot{z})\theta - K_c \Delta\dot{\tilde{z}} \tag{28}$$

which with known true parameters, θ, results in the controlled system dynamics of

$$\Delta\ddot{z} = \begin{bmatrix} \Delta\ddot{\tilde{z}} \\ \ddot{y} \end{bmatrix} = \begin{bmatrix} -\overline{M}^{-1}(\theta)\overline{B}A(\theta)K_c\Delta\dot{\tilde{z}} \\ -\frac{C_\Sigma}{m\dot{x}}\dot{y} - \frac{C_\Delta l}{m\dot{x}}\dot{\psi} + \frac{C_{\alpha f}}{m}\delta - \dot{x}\dot{\psi} \end{bmatrix}. \tag{29}$$

The error dynamics of $\Delta\ddot{\tilde{z}} = -\overline{M}^{-1}(\theta)\overline{B}A(\theta)K_c\Delta\dot{\tilde{z}}$ are exponentially stable at $\Delta\ddot{\tilde{z}} = 0$ because $-\overline{M}^{-1}(\theta)\overline{B}A(\theta)K_c$ is a diagonal matrix whose negative entries are its eigenvalues and, moreover, $\Delta x(t)$ and $\Delta\psi(t)$ are decoupled (non-interacting).

The smooth, continuous, bounded reference signals, $\dot{\tilde{z}}_d$ and $\ddot{\tilde{z}}_d$, arguments in Section III-F guarantee that $\forall \epsilon > 0,\ \dot{x}(t) \geq \epsilon\ \forall\ t \geq 0$, and the VTC system (29) provides asymptotic convergence of $\Delta\dot{\tilde{z}}$ to 0 and boundedness of all signals.

C. A Novel Adaptive Velocity Tracking Controller (AVTC)

This Section reports a novel adaptive model-based AVTC, (III-B), for the ground vehicle plant (9) (also (12)) that does not require exact knowledge of the true parameter vector θ that is required by the non-adaptive model-based VTC (23), provides for asymptotic convergence of $\Delta\dot{\tilde{z}} \triangleq [\Delta\dot{x}\ \Delta\dot{\psi}]^T$ to zero and boundedness of all signals. The AVTC takes a form similar to (28) of

$$u = \hat{A}^{-1}\overline{B}^{-1}W_c(\ddot{\tilde{z}}_d, \dot{z})\hat{\theta} - K_c\Delta\dot{\tilde{z}} \tag{30}$$

where $\hat{\theta}(t) \in \mathbb{R}^7$ is an adaptive estimate of the true parameter vector θ, and $\hat{A}^{-1} = A(\hat{\theta}(t))^{-1}$ where $A : \mathbb{R}^7 \rightarrow \mathbb{R}^{2\times2}$ is defined in (14). In the sequel for simplicity we will denote $A = A(\theta)$, and $\overline{M} = \overline{M}(\theta)$.

The AVTC parameter update law takes the form

$$\dot{\hat{\theta}} = \Delta\dot{\theta} \triangleq -\Lambda\mathbb{W}_z(\ddot{\tilde{z}}_d, \dot{z}, \hat{\theta})^T\Delta\dot{\tilde{z}} \tag{31}$$

where $\mathbb{W}_z(\ddot{\tilde{z}}_d, \dot{z}, \hat{\theta})$ is defined in (36) and $\Lambda \in \mathbb{R}^{7\times7}$ is a PDD parameter adaptation gain matrix. Larger Λ causes faster parameter convergence. Defining error coordinates

$$\Delta\theta \triangleq \hat{\theta} - \theta \quad \text{and} \quad \Delta A \triangleq \hat{A} - A, \tag{32}$$

and noting the property $A\hat{A}^{-1} = I - \Delta A\hat{A}^{-1}$, the controller (30) and the plant error dynamics (22) result in AVTC closed loop system error dynamics of

$$\overline{M}\Delta\ddot{\tilde{z}} = W_c(\ddot{\tilde{z}}_d, \dot{z})\Delta\theta - \Delta A\hat{A}^{-1}W_c(\ddot{\tilde{z}}_d, \dot{z})\hat{\theta} - \overline{B}AK_c\Delta\dot{\tilde{z}}. \tag{33}$$

Defining a new regressor

$$W_\Delta(\ddot{\tilde{z}}_d, \dot{z}, \hat{\theta}) \triangleq D_{\Delta\theta}[\Delta A\hat{A}^{-1}W_c(\ddot{\tilde{z}}_d, \dot{z})\hat{\theta}], \tag{34}$$

and substituting $\hat{\theta} = \theta + \Delta\theta$ into (33) yields

$$\overline{M}\Delta\ddot{\tilde{z}} = [W_c(\ddot{\tilde{z}}_d, \dot{z}) - W_\Delta(\ddot{\tilde{z}}_d, \dot{z}, \hat{\theta})]\Delta\theta - \overline{B}AK_c\Delta\dot{\tilde{z}} \tag{35}$$

which can be simplified by defining $\mathbb{W}_z(\ddot{\tilde{z}}_d, \dot{z}, \hat{\theta}) \in \mathbb{R}^{2\times7}$ as

$$\mathbb{W}_z(\ddot{\tilde{z}}_d, \dot{z}, \hat{\theta}) \triangleq W_c(\ddot{\tilde{z}}_d, \dot{z}) - W_\Delta(\ddot{\tilde{z}}_d, \dot{z}, \hat{\theta}). \tag{36}$$

The regressor $\mathbb{W}_z(\ddot{\tilde{z}}_d, \dot{z}, \hat{\theta})$ (36) takes the explicit form

$$\mathbb{W}_z = \begin{bmatrix} \ddot{x}_d - \dot{\psi}\dot{y} & 0 & \alpha_1 & \dot{x} & 0 & 0 & 0 \\ 0 & \ddot{\psi}_d & 0 & 0 & \alpha_2 & \frac{l^2\dot{\psi}}{\dot{x}} & \frac{l\dot{y}}{\dot{x}} \end{bmatrix} \tag{37}$$

where the α_i are

$$\alpha_1 = -\hat{K}_t^{-1}(\hat{C}_{rr}\dot{x} + \hat{m}(\ddot{x}_d - \dot{\psi}\dot{y})) \tag{38}$$

$$\alpha_2 = -(\hat{C}_{\alpha f}\ddot{x})^{-1}(\hat{C}_\Sigma\dot{\psi}l^2 + \hat{C}_\Delta\dot{y}l + \hat{J}_z\ddot{\psi}_d\dot{x})$$

Substituting (36) into (35) results in AVTC controlled system error dynamics of

$$\Delta\ddot{\tilde{z}} = \overline{M}^{-1}[\mathbb{W}_z(\ddot{\tilde{z}}_d, \dot{z}, \hat{\theta})\Delta\theta - \overline{B}AK_c\Delta\dot{\tilde{z}}] \tag{39}$$

thus identical to non-adaptive VTC error dynamics (29) if

$$0 = \mathbb{W}_z(\ddot{\tilde{z}}_d, \dot{z}, \hat{\theta})\Delta\theta. \tag{40}$$

D. Equivalence of VTC and AVTC

This Section reports the requirements the estimated parameter vector, $\hat{\theta}$, must meet for the AVTC controller to produce the same dynamics as the non-adaptive model-based VTC with known parameters. It is easy to show by direct computation that $\hat{\theta}$ is in the persistent nullspace of $\mathbb{W}_z(\ddot{\tilde{z}}_d, \dot{z}, \hat{\theta})$, i.e. $\hat{\theta} \in \text{null}(\mathbb{W}_z(\ddot{\tilde{z}}_d, \dot{z}, \hat{\theta}))$, thus (40) simplifies to

$$0 = \mathbb{W}_z(\ddot{\tilde{z}}_d, \dot{z}, \hat{\theta})\theta. \tag{41}$$

Substituting (41) into (39) and multiplying by $\hat{A}$ yields

$$\hat{A}\Delta\ddot{\tilde{z}} = \overline{M}^{-1}[\hat{A}\mathbb{W}_z(\ddot{\tilde{z}}_d, \dot{z}, \hat{\theta})\theta - \hat{A}\overline{B}AK_c\Delta\dot{\tilde{z}}]. \tag{42}$$

Using the Jacobian operator to define

$$W_\theta(\ddot{\tilde{z}}_d, \dot{z}, \theta) \triangleq D_{\hat{\theta}}[\hat{A}\mathbb{W}_z(\ddot{\tilde{z}}_d, \dot{z}, \hat{\theta})\theta] \tag{43}$$

we can rewrite (42) as

$$\hat{A}\Delta\ddot{\tilde{z}} = \overline{M}^{-1}[W_\theta(\ddot{\tilde{z}}_d, \dot{z}, \theta)\hat{\theta} - \hat{A}\overline{B}AK_c\Delta\dot{\tilde{z}}]. \tag{44}$$

Finally, we can show that if $\hat{\theta}$ is in the persistent nullspace of $W_\theta(\ddot{\tilde{z}}_d, \dot{z}, \theta)$, i.e. $0 = W_\theta(\ddot{\tilde{z}}_d, \dot{z}, \theta)\hat{\theta}$, then the AVTC system error dynamics will take the form

$$\hat{A}\Delta\ddot{\tilde{z}} = -\overline{M}^{-1}\hat{A}\overline{B}AK_c\Delta\dot{\tilde{z}} \tag{45}$$

$$\Delta\ddot{\tilde{z}} = -\overline{M}^{-1}\overline{B}AK_c\Delta\dot{\tilde{z}} \tag{46}$$

which is identical to the VTC error dynamics (29).

$W_\theta(\ddot{\tilde{z}}_d, \dot{z}, \theta)$, also denoted as W_θ, takes the form

$$\begin{bmatrix} \beta_1 & 0 & \beta_2 & -K_t\dot{x} & 0 & 0 & 0 \\ 0 & -C_{\alpha f}\ddot{\psi}_d & 0 & 0 & \beta_3 & -\frac{C_{\alpha f}l^2\dot{\psi}}{\dot{x}} & -\frac{C_{\alpha f}l\dot{y}}{\dot{x}} \end{bmatrix} \tag{47}$$

where β_1, β_2 and β_3 are defined as

$$\beta_1 = -K_t(\ddot{x}_d - \dot{\psi}\dot{y}) \tag{48}$$

$$\beta_2 = C_{rr}\dot{x} + m\ddot{x}_d - m\dot{\psi}\dot{y} \tag{49}$$

$$\beta_3 = \dot{x}^{-1}(C_\Sigma\dot{\psi}l^2 + C_\Delta\dot{y}l + J_z\ddot{\psi}_d\dot{x}). \tag{50}$$

Similar to (37), W_θ has a persistent nullity of 2, where the nullspace can be represented as the span of linear combinations of vectors that contain the true parameter values

$$\text{null}(W_\theta) = \text{span}\left\{\begin{bmatrix} m & 0 & K_t & C_{rr} & 0 & 0 & 0 \end{bmatrix}^T, \begin{bmatrix} 0 & J_z & 0 & 0 & C_{\alpha f} & C_\Sigma & C_\Delta \end{bmatrix}^T\right\} \tag{51}$$

and any nonzero linear combination of $\hat{\theta}$ such that $\hat{\theta} \in \text{null}(W_\theta(\ddot{\tilde{z}}_d, \dot{z}, \theta))$ will result in asymptotically stable velocity tracking of continuous, smooth, bounded $\dot{x}_d(t)$ and $\dot{\psi}_d(t)$ signals, identical to the VTC in III-B. As reported in [7], the 'true' parameter values needed for ideal controller performance include not just one set of values, θ, they can be any element θ^* of the set $P(\theta)$ defined as

$$P(\theta) \triangleq \{\theta^* \in \mathbb{R}^{7\times1} : W_\theta(\ddot{\tilde{z}}_d, \dot{z}, \theta)\theta^* = 0\}. \tag{52}$$

E. AVTC Controller Lyapunov Stability Analysis

This Section reports a Lyapunov stability proof for the AVTC ground vehicle controller. With the AVTC controller dynamics (39), the full system error dynamics are

$$\Delta\ddot{z} = \begin{bmatrix} \Delta\ddot{\tilde{z}} \\ \ddot{y} \end{bmatrix} = \begin{bmatrix} -\overline{M}^{-1}[\mathbb{W}_z(\ddot{\tilde{z}}_d, \dot{z}, \hat{\theta})\Delta\theta - \overline{B}AK_c\Delta\dot{\tilde{z}}] \\ -\frac{C_\Sigma}{m\dot{x}}\dot{y} - \frac{C_\Delta l}{m\dot{x}}\dot{\psi} + \frac{C_{\alpha f}}{m}\delta - \dot{x}\dot{\psi} \end{bmatrix} \tag{53}$$

where $\Delta\ddot{z}$, $\Delta\ddot{\tilde{z}}$, $\ddot{\tilde{z}}$ and $\dot{z}$ are defined in (20), (21), (9) and (8).

Given a smooth bounded reference velocity and acceleration signals, $\dot{\tilde{z}}_d$ and $\ddot{\tilde{z}}_d$, the Lyapunov function of $\Delta\dot{\tilde{z}}$ and $\Delta\theta$ is

$$V(\Delta\dot{\tilde{z}}, \Delta\theta) = \frac{1}{2}\Delta\dot{\tilde{z}}^T\overline{M}\Delta\dot{\tilde{z}} + \frac{1}{2}\Delta\theta^T\Lambda^{-1}\Delta\theta \tag{54}$$

where $\Lambda \in \mathbb{R}^{7\times7}$ is the PDD adaptation gain matrix from (31). $V(\Delta\dot{\tilde{z}}, \Delta\theta) \in C^1$, positive definite, and radially unbounded.

The time derivative of $V(\Delta\dot{\tilde{z}}, \Delta\theta)$ is

$$\dot{V}(\Delta\dot{\tilde{z}}, \Delta\theta) = \Delta\dot{\tilde{z}}^T\overline{M}\Delta\ddot{\tilde{z}} + \Delta\theta^T\Lambda^{-1}\Delta\dot{\theta}. \tag{55}$$

Substituting $\Delta\ddot{\tilde{z}}$ from (39) yields

$$\dot{V} = \Delta\dot{\tilde{z}}^T[\mathbb{W}_z(\ddot{\tilde{z}}_d, \dot{z}, \hat{\theta})\Delta\theta - \overline{B}AK_c\Delta\dot{\tilde{z}}] + \Delta\theta^T\Lambda^{-1}\Delta\dot{\theta}. \tag{56}$$

Substituting the parameter update law (31) into (56) yields

$$\dot{V}(\Delta\dot{\tilde{z}}, \Delta\theta) = -\Delta\dot{\tilde{z}}^T\overline{B}AK_c\Delta\dot{\tilde{z}} \leq 0, \tag{57}$$

which is negative definite in $\Delta\dot{\tilde{z}}$, and negative semi-definite in the full error state $(\Delta\dot{\tilde{z}}, \Delta\theta)$.

Given that $V(\Delta\dot{\tilde{z}}, \Delta\theta)$, (54), is a continuous and radially unbounded function of $\Delta\dot{\tilde{z}}$ and $\Delta\theta$, is bounded below by zero and, in consequence of (57) is bounded above by its initial

value, $\Delta\dot{\tilde{z}}$ and $\Delta\theta$ are bounded, i.e. $\in \mathcal{L}^\infty$. The boundedness of $\Delta\dot{\tilde{z}}$ and $\Delta\theta$, (21) and (32), and the boundedness of $\dot{\tilde{z}}_d$ and θ imply that $\dot{z}$, $\hat{\theta}$, and $\hat{A}$ are $\in \mathcal{L}^\infty$.

Section III-F shows that for sufficiently small initial conditions $\Delta\dot{\tilde{z}}(0)$ and $\Delta\theta(0)$, $\dot{x}(t)$ is bounded below by a positive constant, thus the $\dot{x}(t)^{-1}$ terms appearing in $W_c(\ddot{\tilde{z}}_d, \dot{z})$ in (30) are defined and bounded. Section (III-G) shows that for sufficiently small initial conditions all parameter estimate terms, $\hat{\theta}_i(t)$, (10), are bounded below by a positive constant. Given that all terms on the right hand side of (30) and (39) are bounded, the signals $u(t)$ and $\Delta\ddot{\tilde{z}}$ are $\in \mathcal{L}^\infty$.

Denoting $\alpha_{min} > 0$ as the minimum entry (and eigenvalue) of the PDD matrix $\overline{B}AK_c \in \mathbb{R}^{2\times 2}$ appearing in (57) we have

$$\int_0^\infty |\Delta\dot{\tilde{z}}(\tau)|^2 d\tau \leq \int_0^\infty \alpha_{min}^{-1}\dot{V}(\tau)d\tau \leq \alpha_{min}^{-1}(V(\infty) - V(0)). \tag{58}$$

Thus $\Delta\dot{\tilde{z}}(t) \in \mathcal{L}^2 \bigcap \mathcal{L}^\infty$ and $\Delta\ddot{\tilde{z}} \in \mathcal{L}^\infty$, and from Corollary 2.9 of [17] we can conclude $\lim_{t\to\infty} \Delta\dot{\tilde{z}}(t) = 0$.

The asymptotic convergence of $\Delta\dot{\tilde{z}}(t)$ to zero and the boundedness of all other terms of the parameter update law (31) implies that $\lim_{t\to\infty} \dot{\hat{\theta}}(t) = 0$.

F. Boundedness of Longitudinal Velocity $\dot{x}(t)$

This Section reports a proof showing that given the controlled system dynamics in (53), for any $\epsilon > 0$ there exists a local set of initial conditions of $\Delta\dot{\tilde{z}}$ and $\Delta\theta$ and a reference signal bound $\dot{x}_d(t) \geq 2\epsilon\ \forall t \geq 0$, where ϵ is a positive constant, such that the longitudinal velocity will remain positive and bounded below, $\dot{x}(t) > \epsilon\ \forall t \geq 0$. This argument is necessary to conclude that all signals in (9), (30), (31), and (53) are bounded, which is a requirement for the Lyapunov stability analysis in Section III-E.

If the initial condition of $\Delta\dot{\tilde{z}}(0)$ and $\Delta\theta(0)$ are such that

$$V(\Delta\dot{\tilde{z}}(0), \Delta\theta(0)) \leq \frac{1}{2}m\epsilon^2 \tag{59}$$

then from (57), it follows that

$$V(\Delta\dot{\tilde{z}}, \Delta\theta) \leq \frac{1}{2}m\epsilon^2 \quad \forall t \geq 0. \tag{60}$$

From (54) and (59) we have

$$\frac{1}{2}\Delta\dot{\tilde{z}}^T\overline{M}\Delta\dot{\tilde{z}} + \frac{1}{2}\Delta\theta^T\Lambda^{-1}\Delta\theta \leq \frac{1}{2}m\epsilon^2. \tag{61}$$

Expanding the terms in $\Delta\dot{\tilde{z}}$ results in

$$\frac{1}{2}m\Delta\dot{x}^2 + \frac{1}{2}J_z\Delta\dot{\psi}^2 + \frac{1}{2}\Delta\theta^T\Lambda^{-1}\Delta\theta \leq V(\Delta\dot{\tilde{z}}(0), \Delta\theta(0)) \leq \frac{1}{2}m\epsilon^2, \tag{62}$$

$$\Delta\dot{x}^2 \leq \epsilon^2, \tag{63}$$

thus

$$|\dot{x} - \dot{x}_d| \leq \epsilon. \tag{64}$$

Either $\dot{x}_d \geq \dot{x}$ or $\dot{x}_d \leq \dot{x}$. In the case of $\dot{x}_d > \dot{x}$, then

$$\dot{x}_d - \dot{x} \leq \epsilon \tag{65}$$

$$-\dot{x} \leq \epsilon - \dot{x}_d \tag{66}$$

$$\dot{x} \geq \dot{x}_d - \epsilon. \tag{67}$$

If the following condition is satisfied by the reference signal

$$\dot{x}_d(t) \geq 2\epsilon \quad \forall t \geq 0 \tag{68}$$

then $\dot{x}(t) \geq \epsilon \quad \forall t \geq 0$. If $\dot{x}_d \leq \dot{x}$, (68) ensures that

$$\dot{x}(t) \geq 2\epsilon \quad \forall t \geq 0, \tag{69}$$

thus we conclude if the initial conditions in (59) and the reference signal condition in (68) are satisfied, then $\dot{x}(t) > \epsilon$.

G. Boundedness of Parameter Estimate $\theta(t)$

This Section reports a proof showing that if the initial conditions $\Delta\dot{\tilde{z}}$ and $\Delta\theta$ are sufficiently small then the elements of the parameter estimate $\hat{\theta}(t)$ appearing in $\hat{A}^{-1}$ in (30) will remain positive and bounded below. This ensures that $\hat{A}^{-1}$ exists and is bounded, and the control signal $u(t)$ is bounded.

Denoting $\lambda_i > 0$ as the diagonal entries in the PDD matrix Λ in (31), $\lambda_{min} > 0$ as the minimum diagonal entry (and thus the minimum eigenvalue) of Λ, and $\theta_{min} > 0$ as the minimum of the absolute values of each of the elements in the parameter vector θ (10), if the initial conditions of $\Delta\dot{\tilde{z}}(t)$ and $\Delta\theta$ of the Lyapunov function in (54) are such that

$$V(\Delta\dot{\tilde{z}}(0), \Delta\theta(0)) \leq \frac{1}{2}\lambda_{min}^{-1}(\frac{\theta_{min}}{2})^2 \tag{70}$$

it follows that

$$V(\Delta\dot{\tilde{z}}, \Delta\theta) \leq \frac{1}{2}\lambda_{min}^{-1}(\frac{\theta_{min}}{2})^2 \quad \forall t \geq 0 \tag{71}$$

Expanding the $\Delta\theta$ terms in $V(\Delta\dot{\tilde{z}}, \Delta\theta)$ results in

$$V(\Delta\dot{\tilde{z}}, \Delta\theta) = \frac{1}{2}\Delta\dot{\tilde{z}}^T\overline{M}\Delta\dot{\tilde{z}} + \sum_{i=1}^{7}\frac{1}{2}\lambda_i^{-1}\Delta\theta_i^2 \leq \frac{1}{2}\lambda_{min}^{-1}(\frac{\theta_{min}}{2})^2 \tag{72}$$

thus $\forall i \in \{1...7\}$

$$\frac{1}{2}\lambda_i^{-1}\Delta\theta_i^2 \leq \frac{1}{2}\lambda_{min}^{-1}(\frac{\theta_{min}}{2})^2. \tag{73}$$

and since $\lambda_{min} \leq \lambda_i$

$$\frac{1}{2}\lambda_{min}^{-1}\Delta\theta_i^2 \leq \frac{1}{2}\lambda_{min}^{-1}(\frac{\theta_{min}}{2})^2 \tag{74}$$

$$\Delta\theta_i^2 \leq (\frac{\theta_{min}}{2})^2 \tag{75}$$

$$|\Delta\theta_i| \leq \frac{\theta_{min}}{2}. \tag{76}$$

Recalling from (32) that $\Delta\theta_1(t) = \hat{\theta}_i(t) - \theta_i$, thus the $\theta_i(t)$ are all positive and bounded below

$$\hat{\theta}_i(t) \geq \frac{\theta_{min}}{2}. \tag{77}$$

This property guarantees that the term $\hat{A}^{-1}$ appearing in (30) exists and is positive and bounded and, with the boundedness the other terms of (30), guarantees that $u(t)$ is bounded.

IV. AVTC Controller Simulation Evaluation

This Section reports simulation evaluation of AVTC control (30) (31) in comparison to VTC, Velocity Tracking Controller with Integral Feedback (VTC-I), and Active Disturbance Rejection Controller (ADRC). VTC-I takes the form

$$u = A^{-1}(\theta)\overline{B}^{-1}W_c(\ddot{\tilde{z}}_d, \dot{z})\theta - K_c\Delta\dot{\tilde{z}} - K_i\int_0^t \Delta\dot{\tilde{z}}(\tau)d\tau \tag{78}$$

where $K_c = \text{diag}\left(\begin{bmatrix}0.8,\ 0.7\end{bmatrix}\right)$ and $K_i = \text{diag}\left(\begin{bmatrix}0.9,\ 1.2\end{bmatrix}\right)$ are the proportional and integral feedback gains, respectively. The ADRC velocity tracking controller used herein follows the design of [6]. Using the notation of [6], the observer states for velocity tracking are $z_2 \in \mathbb{R}^2$ and $z_3 \in \mathbb{R}^2$. The observer state update laws take the form $\dot{z}_2 = z_3 + b_0u - \beta_{02}fe$ and $\dot{z}_3 = -\beta_{03}fe_1$ where the gains are defined as $\beta_{02} = \text{diag}\left(\begin{bmatrix}10,\ 10\end{bmatrix}\right)$, $\beta_{03} = \text{diag}\left(\begin{bmatrix}20,\ 20\end{bmatrix}\right)$, and $b_0 = \text{diag}\left(\begin{bmatrix}\hat{K}_t,\ l\ \hat{C}_{\alpha f}\end{bmatrix}\right)$. The error terms are defined as $fe = fal(e, 0.5, 0.5)$, $fe_1 = fal(e, 0.25, 0.5)$, and $e = z_2 - \dot{\tilde{z}}_d$

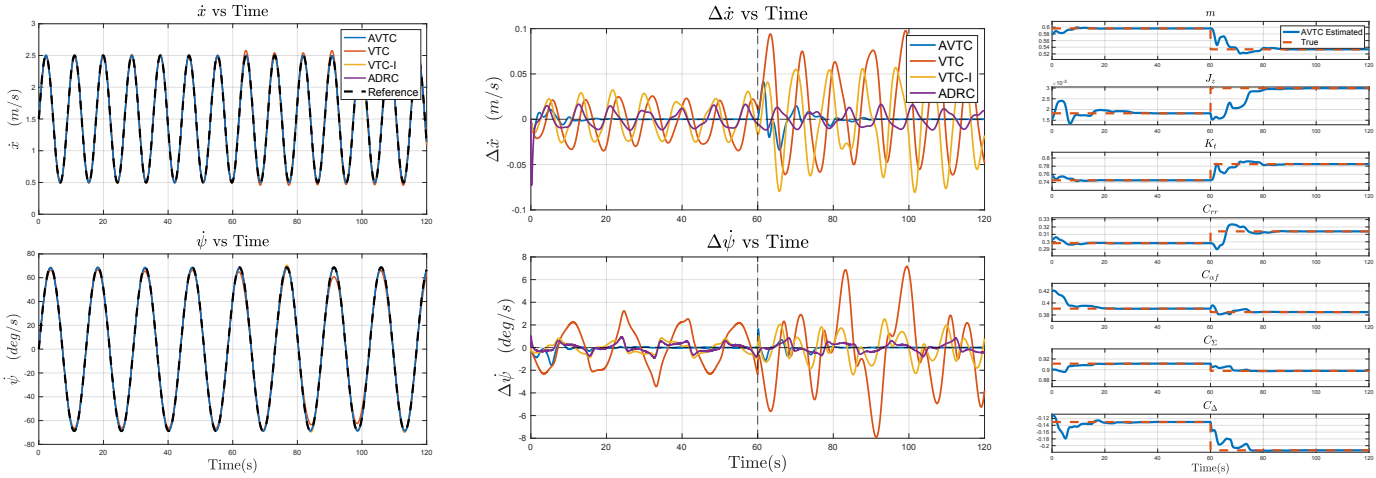

(a) Actual and reference vehicle velocities vs time.

(b) Velocity tracking error vs time showing asymptotically exact AVTC tracking.

(c) Normalized AVTC parameter estimates vs time.

Fig. 1: Simulation: AVTC performance evaluation and comparison to VTC, Velocity Tracking Controller with Integral Feedback (VTC-I), and Active Disturbance Rejection Controller (ADRC). Vehicle "true" parameters change at $t = 60s$ to simulate two simultaneous parametric faults arising from changes in surface conditions and payload.

TABLE III: Simulation Reference Velocities

$\dot{x}_d(t) = 1.5 + 1.0\sin(0.71t)$	m/s
$\dot{\psi}_d(t) = 1.2\sin(0.43t)$	rad/s

TABLE IV: Simulation Tracking Comparison

	Controller	$\Delta\dot{x}(t)$ RMS (m/s)	$\Delta\dot{\psi}(t)$ RMS (rad/s)
Steady-state $90s < t < 120s$	AVTC	**0.0001**	**0.0001**
	VTC	0.0344	0.0417
	VTC-I	0.0293	0.0145
	ADRC	0.0098	0.0064

where $fal(e, \alpha, \delta)$ is the fractional power function defined in [6]. The virtual control input, u_0 and control input, u, is computed as $u_0 = \dddot{\tilde{z}}_d - k_{adrc}\Delta\dot{\tilde{z}}$ and $u = b_0^{-1}(u_0 - z_3)$ with controller gain, $k_{adrc} = \text{diag}\left(\begin{bmatrix}100, & 25\end{bmatrix}\right)$. Table III gives the reference velocities used for the simulation of our 1/10 scale vehicle, whose peak velocities of 2.5 m/s correspond to full-scale vehicle peak velocities of 25 m/s (90 km/h). Sinusoidal variation of reference velocities is employed because Persistence of Excitation (PE) of the regressor signals is known to improve parameter convergence [7], [17]. The true parameter vector, $\theta = [4, 0.07, 5, 2, 15, 35, -5]^T$ and adaptation gain matrix, $\Lambda = \text{diag}\left([1, 1.5, 0.5, 0.1, 50, 10, 500]\right)$ were used for the simulation.

The 120 second simulation was computed with `ODE45` in MATLAB. The estimated parameters $\hat{\theta}(t)$ were initialized at $t = 0$ to +/-20% of the true parameter values. At $t = 60s$ two simultaneous faults were simulated: the tire slip parameters were reduced by 40% to simulate change in surface conditions and the vehicle mass was decreased by 15% to simulate change in vehicle payload.

Fig. 1a shows the simulated vehicle velocity and reference signal and Fig. 1b shows the simulated vehicle velocity tracking error converging asymptotically to zero, corroborating the stability proof in III-E. Fig. 1c shows the normalized AVTC parameter estimates to converge to the normalized true parameter set $P(\theta)$ defined in (52). AVTC thus provides real-time fault detection and fault-tolerant control. Table IV compares the Root Mean Squared (RMS) velocity tracking error for the AVTC, VTC, VTC-I, and ADRC controllers.

Additional simulations, not shown herein due to page limits, demonstrated that AVTC achieves asymptotically stable tracking of the reference velocities and parameter convergence to the true parameter set when every element in the initial parameter estimate was initialized to a value within $\pm 50\%$ of the true parameter values or when any single element in the initial parameter estimate was initialized to a value within $\pm 700\%$ of the true parameter value.

Parameter vectors θ and $\hat{\theta}$ are normalized hereafter to facilitate visualization and comparison of the parameter estimates. Normalization requires separating the parameter vector into two distinct components, $\theta_{\dot{x}}$ and $\theta_{\dot{\psi}}$, defined as

$$\theta_{\dot{x}} = \begin{bmatrix} m & K_t & C_{rr} \end{bmatrix}^T, \ \theta_{\dot{\psi}} = \begin{bmatrix} J_z & C_{\alpha f} & C_\Sigma & C_\Delta \end{bmatrix}^T \tag{79}$$

and normalizing each data point i, to obtain $\tilde{\theta}_{\dot{x}i}$ and $\tilde{\theta}_{\dot{\psi}i}$ as

$$\tilde{\theta}_{\dot{x}i} = \frac{\theta_{\dot{x}i}}{||\theta_{\dot{x}i}||_2}, \quad \tilde{\theta}_{\dot{\psi}i} = \frac{\theta_{\dot{\psi}i}}{||\theta_{\dot{\psi}i}||_2}. \tag{80}$$

The simulation results corroborate the stability proof of the AVTC in Section III-E and in addition, show the parameter estimates converging to the true parameter set defined in (52).

V. AVTC Controller Experimental Evaluation

This Section reports an experimental evaluation of AVTC performance. Section V-A describes the experimental setup. Section V-B reports the experimental performance results.

A. Ground Vehicle Experimental Setup

We used a brushless computer-controlled 1/10th scale model vehicle for the experimental evaluation, Fig. 2. The vehicle mass was 4.378 kg, the length from front to rear axle was 0.28 m, and the center of gravity was located in the longitudinal center of the vehicle such that $l = 0.14$ m. A Vedder's Electronic Speed Controller (VESC Project, B. Vedder) was used so that servo pulse commands were linearly proportional

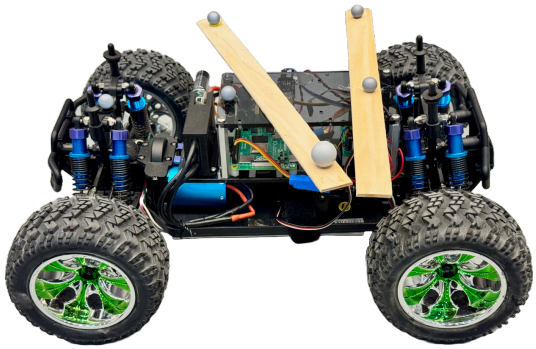

Fig. 2: Experimental Ground Vehicle

TABLE V: Experimental Reference Velocities

Trial 1	$\dot{x}_d(t) = 1.05$	m/s
Constant Yaw Rate	$\dot{\psi}_d(t) = 1.1$	rad/s
Trial 2	$\dot{x}_d(t) = 1.5 + 0.1\sin(0.71t)$	m/s
Sinusoidal Yaw Rate	$\dot{\psi}_d(t) = 1.2 + 0.1\sin(0.43t)$	rad/s

to a motor current, I_m [A], between -15 and +15 [A] . Vehicle steering, δ [rad], was controlled with servo pulse commands to the front wheel steering servo.

The experiments were conducted in a laboratory outfitted with a Qualisys 7+ Series Motion Capture System (Qualisys, Goteborg, Sweden) with an operational area of 9.7 m x 6.7 m. The lab's motion capture system provided vehicle position and orientation data at 50 Hz. The position signals were differentiated and converted to the vehicle body-frame to provide the $\dot{x}(t)$, $\dot{\psi}(t)$ and $\dot{y}(t)$ velocity signals at 50 Hz.

Though a more complex reference velocity trajectory similar to that employed in the numerical simulation in Section IV is preferred, the experimental evaluation reference signals were simplified to ensure that the vehicle would stay inside of the motion capture operational area. Table V defines the experimental reference velocities, whose peak velocities of 1.6 m/s correspond to full-scale velocities of 16 m/s (57.6 km/h).

All four controllers, AVTC (30), Non-adaptive VTC (28), VTC-I (78), and ADRC [6], were implemented in Python running on a Raspberry Pi 4 Model B (Raspberry Pi Ltd, Cambridge, England), which sent the servo pulse commands to the VESC and steering servo. All controllers used the same initial parameter vector, $\hat{\theta} = [4.378 \quad 0.0715 \quad 7.0 \quad 2.0 \quad 20.0 \quad 30.0 \quad 10.0]^T$ with the vehicle at a standstill at the beginning of each experiment. In order to avoid a division by zero error, a constant 15A signal was sent to the motor until the vehicle reached a minimum longitudinal velocity of 0.1 m/s. The vehicle was then controlled with each controller for 120 seconds. The 50 Hz data was logged and plotted without any post-processing.

B. AVTC Controller Experimental Evaluation

The AVTC controller gain (30) was set to $K_c = \text{diag}([0.9,\ 0.6])$ and the parameter update law (31) used the adaption gain $\Lambda = \text{diag}([0.5,\ 0.01,\ 0.5,\ 0.1,\ 100,\ 20,\ 20])$.

Fig. 3a shows the Experimental Ground Vehicle sinusoidal longitudinal velocity and yaw rate tracking performance with the AVTC, Non-adaptive VTC, VTC-I, and ADRC controllers. Fig. 3b shows the corresponding velocity tracking error, and Table VI compares the RMS velocity error for the final 30 seconds of the experimental trial to evaluate the steady-state performance of the controllers. Fig. 3c shows the normalized parameter estimates for the AVTC controller during the trial.

TABLE VI: Experimental Tracking Comparison

	Controller	$\Delta\dot{x}(t)$ RMS (m/s)	$\Delta\dot{\psi}(t)$ RMS (rad/s)
Steady-state $90s < t < 120s$	AVTC	**0.0282**	**0.0388**
	VTC	0.2983	0.1709
	VTC-I	0.0844	0.0501
	ADRC	0.0324	0.0405

The experimental data show that the AVTC velocity tracking error converges near zero, as expected from the Lyapunov stability analysis of Section III-E. The parameter estimates converge to constant values within 80 seconds. Table VII compares the initial and final normalized parameter values. Note that most of the "true" parameters are unknown.

TABLE VII: AVTC Experimental Parameter Estimates

Parameter	Initial $\hat{\theta}$	Final $\hat{\theta}$	Units
m	4.38	3.72	kg
J_z	0.0715	0.0717	$kg \cdot m^2$
K_t	7.0	10.2	N/A
C_{rr}	2.0	1.46	$N \cdot s/m$
$C_{\alpha f}$	20.0	9.05	N/rad
C_Σ	30.0	31.87	N/rad
C_Δ	10.0	6.94	N/rad

VI. Conclusion

This letter reports a novel Adaptive Velocity Tracking Controller (AVTC) for ground vehicles capable of identifying plant and actuator parameters and providing a mathematical proof of asymptotically stable longitudinal and yaw velocity tracking, boundedness of all signals, and convergence of parameter estimates. The AVTC ground vehicle controller is particularly useful for ground vehicles for which exact prior knowledge of vehicle, actuator, and environmental parameters is not available, and for detecting and compensating for real-time faults due to changes in plant, actuator, and environmental parameters. AVTC was evaluated in comparison to its non-adaptive counterpart and two alternative controllers. The analytical, simulation, and experimental results show the following:

1) Non-adaptive VTC and adaptive AVTC are mathematically proven to be stable and provide exact reference-velocity tracking.
2) Adaptive AVTC outperforms non-adaptive VTC and VTC-I for tracking time-varying references when true plant and actuator parameters are unknown, and marginally outperforms ADRC.
3) Adaptive AVTC parameter estimates are shown to converge in a mathematical stability proof, in simulation, and in real-world experiments.
4) Adaptive AVTC robustly detects, quantitatively identifies, and compensates dynamically in real-time for faults arising from changes in plant, actuator, and environmental parameters during operation, and thus provides fault detection and fault-tolerant control.

Acknowledgments

We gratefully acknowledge the scholarly comments and suggestions of the Editor and two anonymous reviewers.

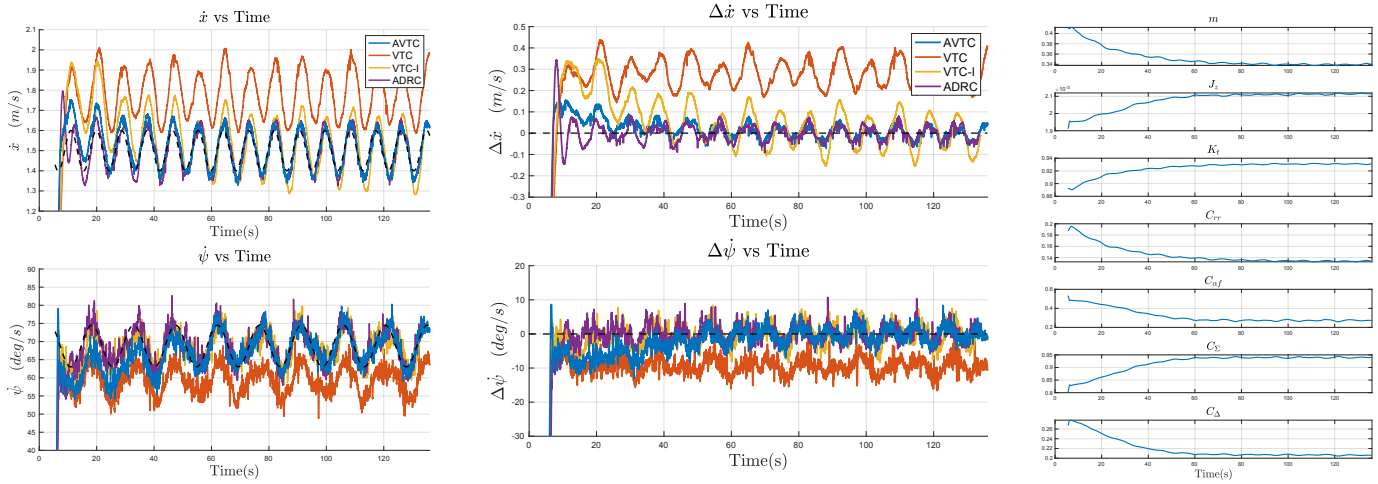

(a) Actual and reference vehicle velocities vs time.

(b) Velocity tracking error vs time.

(c) Normalized AVTC parameter estimates vs time.

Fig. 3: Experiments: AVTC performance evaluation and comparison to VTC, VTC-I, and ADRC.

REFERENCES

[1] C. Ahn, H. Peng, and H. E. Tseng, "Robust estimation of road frictional coefficient," IEEE Trans. Control Systems Technology, vol. 21, no. 1, pp. 1–13, 2013. doi: https://doi.org/10.1109/TCST.2011.2170838

[2] S. Cheng, L. Li, H.-Q. Guo, Z.-G. Chen, and P. Song, "Longitudinal collision avoidance and lateral stability adaptive control system based on MPC of autonomous vehicles," IEEE Trans. on Intelligent Transportation Systems, vol. 21, no. 6, pp. 2376–2385, 2020. doi: https://doi.org/10.1109/TITS.2019.2918176

[3] M. Choi, J. J. Oh, and S. B. Choi, "Linearized recursive least squares methods for real-time identification of tire–road friction coefficient," IEEE Trans. Veh. Tech., vol. 62, no. 7, pp. 2906–2918, 2013. doi: https://doi.org/10.1109/TVT.2013.2260190

[4] T. Devos, I. N. Uva, and F. Naets, "A least-squares identification method for vehicle cornering stiffness identification from common vehicle sensor data," Vehicle System Dynamics, vol. 0, no. 0, pp. 1–21, 2024. doi: https://doi.org/10.1080/00423114.2024.2389212

[5] A. H. Elsberry, J. J. Dawkins, A. M. Mao, and L. L. Whitcomb, "Nullspace adaptive identification of plant and actuator model parameters for underactuated ground vehicles: Theory and experimental evaluation," IFAC-PapersOnLine, vol. 58, no. 28, pp. 1097–1102, 2024, the 4th Modeling, Estimation, and Control Conference – 2024. ISSN 2405-8963. doi: https://doi.org/10.1016/j.ifacol.2025.01.143

[6] J. Han, "From PID to Active Disturbance Rejection Control," IEEE Trans. Industrial Electronics, vol. 56, no. 3, pp. 900–906, 2009. doi: https://doi.org/10.1109/TIE.2008.2011621

[7] Z. J. Harris, A. M. Mao, T. M. Paine, and L. L. Whitcomb, "Stable nullspace adaptive parameter identification of 6 degree-of-freedom plant and actuator models for underactuated vehicles: Theory and experimental evaluation," The Int. Journal of Robotics Research, vol. 42, no. 12, pp. 1070–1093, 2023. doi: https://doi.org/10.1177/02783649231191184

[8] S. Hong, C. Lee, F. Borrelli, and J. K. Hedrick, "A novel approach for vehicle inertial parameter identification using a dual Kalman filter," IEEE Trans. on Intelligent Transportation Systems, vol. 16, no. 1, pp. 151–161, 2015. doi: https://doi.org/10.1109/TITS.2014.2329305

[9] J. Kabzan, L. Hewing, A. Liniger, and M. N. Zeilinger, "Learning-based model predictive control for autonomous racing," IEEE Robotics and Automation Letters, vol. 4, no. 4, pp. 3363–3370, 2019. doi: https://doi.org/10.1109/LRA.2019.2926677

[10] M. B. Khaknejad, R. Kazemi, S. Azadi, and A. Keshavarz, "Identification of vehicle parameters using modified least square method in ADAMS/car," in Proceedings of 2011 International Conference on Modelling, Identification and Control, 2011, pp. 98–103. doi: https://doi.org/10.1109/ICMIC.2011.5973683

[11] S. Kuutti, R. Bowden, Y. Jin, P. Barber, and S. Fallah, "A survey of deep learning applications to autonomous vehicle control," IEEE Tr. Intell. Transportation Systems, vol. 22, no. 2, pp. 712–733, 2021. doi: https://doi.org/10.1109/TITS.2019.2962338

[12] Y. F. Lian, X. Y. Wang, Y. Zhao, and Y. T. Tian, "Direct yaw-moment robust control for electric vehicles based on simplified lateral tire dynamic models and vehicle model," IFAC-PapersOnLine, vol. 48, no. 28, pp. 33–38, 2015, 17th IFAC Symposium on System Identification. ISSN 2405-8963. doi: https://doi.org/https://doi.org/10.1016/j.ifacol.2015.12.096

[13] F. Lin, Y. Chen, Y. Zhao, and S. Wang, "Path tracking of autonomous vehicle based on adaptive model predictive control," Int. J. Adv. Robotic Systems, vol. 16, no. 5, p. 1729881419880089, 2019. doi: https://doi.org/10.1177/1729881419880089

[14] Y. Lin, J. McPhee, and N. L. Azad, "Comparison of deep reinforcement learning and model predictive control for adaptive cruise control," IEEE Tr. Intell. Veh., vol. 6, no. 2, pp. 221–231, 2021. doi: https://doi.org/10.1109/TIV.2020.3012947

[15] A. M. Mao, J. L. Moore, and L. L. Whitcomb, "Nullspace adaptive model-based trajectory-tracking control for a 6-dof underwater vehicle with unknown plant and actuator parameters: Theory and preliminary simulation evaluation," in 2024 IEEE International Conference on Robotics and Automation (ICRA), 2024, pp. 10 436–10 442. doi: https://doi.org/10.1109/ICRA57147.2024.10611318

[16] A. M. Mao and L. L. Whitcomb, "A novel quotient space approach to model-based fault detection and isolation: Theory and preliminary simulation evaluation," in 2021 IEEE/RSJ International Conference on Intelligent Robots and Systems (IROS), 2021, pp. 7119–7126. doi: https://doi.org/10.1109/IROS51168.2021.9636026

[17] K. S. Narendra and A. M. Annaswamy, Stable Adaptive Systems. Dover, 2005.

[18] Ó. Pérez-Gil, R. Barea, E. López-Guillén, L. M. Bergasa, C. Gómez-Huélamo, R. Gutiérrez, and A. Díaz-Díaz, "Deep reinforcement learning based control for autonomous vehicles in CARLA," Multimedia Tools and Applications, vol. 81, no. 3, pp. 3553–3576, 2022. ISBN 1573-7721. doi: https://doi.org/10.1007/s11042-021-11437-3

[19] R. Rajamani, Vehicle Dynamics and Control. Springer US, 2012. doi: https://doi.org/10.1007/978-1-4614-1433-9

[20] G. Reina, M. Paiano, and J.-L. Blanco-Claraco, "Vehicle parameter estimation using a model-based estimator," Mechanical Systems and Signal Processing, vol. 87, pp. 227–241, 2017. ISSN 0888-3270. doi: https://doi.org/10.1016/j.ymssp.2016.06.038

[21] R. Tedrake, Underactuated Robotics, 2023, Course Notes for MIT 6.832. [Online]. Available: https://underactuated.csail.mit.edu

[22] Z. Yu, X. Huang, and J. Wang, "A least-squares regression based method for vehicle yaw moment of inertia estimation," in 2015 American Control Conference (ACC), 2015, pp. 5432–5437. doi: https://doi.org/10.1109/ACC.2015.7172189